Initialization by Measurement of a Superconducting Quantum Bit Circuit

D. Ristè,[1] J. G. van Leeuwen,[1] H.-S. Ku,[2] K. W. Lehnert,[2] and L. DiCarlo[1]

[1]*Kavli Institute of Nanoscience, Delft University of Technology, P.O. Box 5046, 2600 GA Delft, The Netherlands*

[2]*JILA, National Institute of Standards and Technology and the University of Colorado and Department of Physics, University of Colorado, Boulder, Colorado 80309, USA*

(Received 5 April 2012; published 3 August 2012)

We demonstrate initialization by joint measurement of two transmon qubits in 3D circuit quantum electrodynamics. Homodyne detection of cavity transmission is enhanced by Josephson parametric amplification to discriminate the two-qubit ground state from single-qubit excitations nondestructively and with 98.1% fidelity. Measurement and postselection of a steady-state mixture with 4.7% residual excitation per qubit achieve 98.8% fidelity to the ground state, thus outperforming passive initialization.

DOI: 10.1103/PhysRevLett.109.050507 PACS numbers: 03.67.Lx, 42.50.Dv, 42.50.Pq, 85.25.−j

The abilities to initialize, coherently control, and measure a multiqubit register set the overall efficiency of a quantum algorithm [1]. In systems where qubit transition energies significantly exceed the thermal energy, initialization into the ground state can be achieved by waiting several multiples of the qubit relaxation time T_1 [2]. While this passive method has been standard in superconducting qubit systems, recent breakthrough T_1 improvements [3] in circuit quantum electrodynamics (cQED) [4,5] now bring its many shortcomings to light. First, commonly observed [6–8] residual qubit excitations can produce initialization errors exceeding the lowest single- and two-qubit gate errors now achieved ($< 0.3\%$ [3] and $<5\%$ [9], respectively). Second, the wait time between computations grows proportionally with T_1. Third, moving forward, multiple rounds of quantum error correction [10] will be facilitated by reinitializing ancilla qubits fast compared to coherence times.

Active means of initialization currently used in superconducting qubits include microwave sideband cooling [11,12], temporal control [13] of Purcell-enhanced relaxation [14], and coupling to spurious two-level systems [15]. An attractive but challenging alternative is to use a high-fidelity, quantum nondemolition (QND) readout [16] to collapse qubits into known states. QND readout, already demonstrated for trapped ions [17], nitrogen-vacancy centers in diamond [18], and photons [19], also opens the way to real-time quantum feedback [20] and measurement-based quantum computing [1], and facilitates the study of quantum jumps [21,22] and the Zeno effect [23,24]. In cQED, significant progress in this direction has been achieved using bifurcation in nonlinear resonators [25] and parametric amplification [22,26], but T_1 has until now limited the best QND readout fidelity to 86%. Reaching the fault-tolerant threshold for measurement ($\sim 99\%$ fidelity in modern error-correction schemes [27]) remains an outstanding experimental challenge.

In this Letter, we demonstrate high-fidelity, QND joint readout of two superconducting qubits, and use it to perform joint qubit initialization by measurement and postselection. A phase-sensitive Josephson parametric amplifier (JPA) [28,29] significantly enhances the sensitivity of dispersive readout of two long-lived transmon qubits coupled to a 3D microwave cavity [3]. This readout distinguishes the two-qubit ground state from single-qubit excitations with 98.1% fidelity. Up to 99.6% correlation is observed between the measurement result and the post-measurement state, evidencing the quantum nondemolition character. Finally, we demonstrate application of the high-fidelity, nondemolition readout to initialization by measurement. Using postselection, we purify the two-qubit system against a residual excitation of $\sim 4.7\%$ per qubit, achieving probabilistic ground-state preparation with 98.8% fidelity.

Our system consists of an Al 3D cavity enclosing two superconducting transmon qubits, labeled Q_A and Q_B, with transition frequencies $\omega_{A(B)}/2\pi = 5.606(5.327)$ GHz, relaxation times $T_{1A(B)} = 23(27)$ μs, and Ramsey dephasing times $T^*_{2A(B)} = 0.45(4.2)$ μs [30]. The fundamental mode of the cavity (TE101) resonates at $\omega_r/2\pi = 6.548$ GHz (for qubits in ground state) with $\kappa/2\pi = 430$ kHz linewidth, and couples with $g/2\pi \sim 75$ MHz to both qubits. The measured dispersive shifts [5] $2\chi_{A(B)}/2\pi = -3.7(-2.6)$ MHz place the system in the strong dispersive regime of cQED [31].

Qubit readout in cQED typically exploits dispersive interaction with the cavity. A readout pulse is applied at or near resonance with the cavity, and a coherent state builds up in the cavity with amplitude and phase encoding the multiqubit state [5,32]. We optimize readout of Q_A by injecting a microwave pulse through the cavity at $\omega_{RF} = \omega_r - \chi_A$, the average of the resonance frequencies corresponding to qubits in $|00\rangle$ and $|01\rangle$, with left (right) index denoting the state of Q_B (Q_A) [Figs. 1(a) and 1(d)]. This choice maximizes the phase difference between the pointer coherent states. Homodyne detection of the output signal, itself proportional to the intracavity state, is overwhelmed by the noise added by the semiconductor amplifier (HEMT), precluding high-fidelity single-shot readout

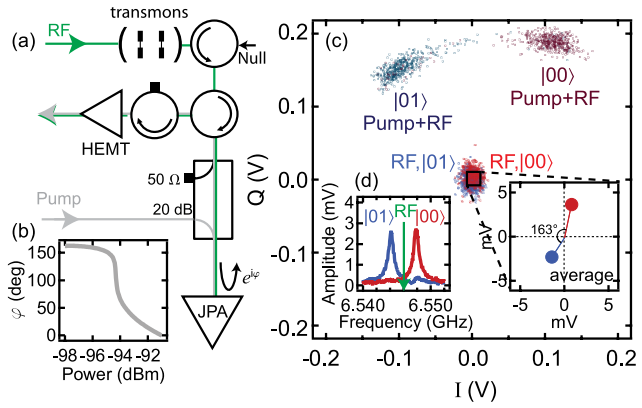

FIG. 1 (color online). JPA-backed dispersive transmon readout. (a) Simplified diagram of the experimental setup, showing the input path for the readout signal carrying the information on the qubit state (RF) and the stronger, degenerate tone (Pump) biasing the JPA. Both microwave tones are combined at the JPA and their sum is reflected with a phase dependent on the total power (b) amplifying the small signal. An additional tone (Null) is used to cancel any pump leakage into the cavity. The JPA is operated at the low-signal gain of ~25 dB and 2 MHz bandwidth. (c) Scatter plot in the I-Q plane for sets of 500 single-shot measurements. Light dots: readout signal obtained with a RF tone probing the cavity for qubits in $|00\rangle$ and $|01\rangle$, respectively. Dark dots: the Pump tone is added to the RF. (d) Spectroscopy of the cavity fundamental mode for qubits in $|00\rangle$ and $|01\rangle$. The RF frequency is chosen halfway between the two resonance peaks, giving the maximum phase contrast (163°; see inset on the right).

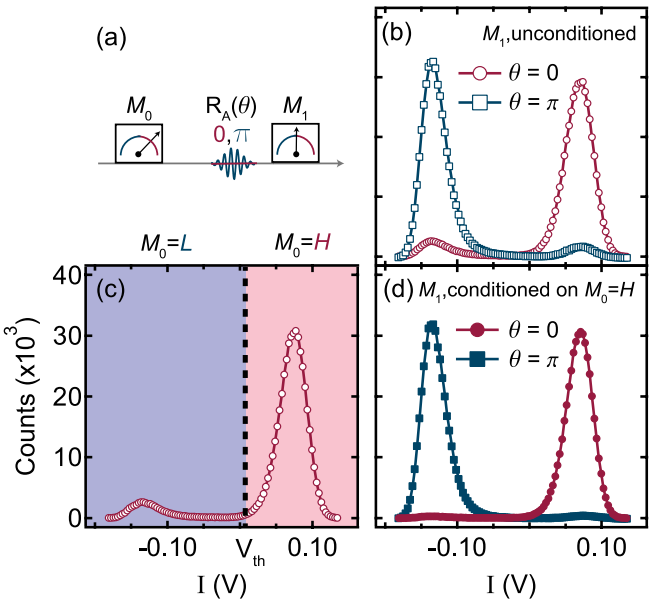

FIG. 2 (color online). Ground-state initialization by measurement. (a) Pulse sequence used to distinguish between the qubit states (M_1), upon conditioning on the result of an initialization measurement M_0. The sequence is repeated every 250 μs. (b) Histograms of 500 000 shots of M_1, without (dots) and with (squares) inverting the population of Q_A with a π pulse. (c) Histograms of M_0, with V_{th} indicating the threshold voltage used to digitize the result. (d) M_1 conditioned on $M_0 = H$ to initialize the system in the ground state, suppressing the residual steady-state excitation. The conditioning threshold, selecting 91% of the shots, matches the value for optimum discrimination of the state of Q_A.

[Fig. 1(c)]. We introduce a JPA [28,33] at the front end of the amplification chain to boost the readout signal by exploiting the power-dependent phase of reflection at the JPA [see Figs. 1(a) and 1(b)]. Depending on the qubit state, the weak signal transmitted through the cavity is either added to or subtracted from a much stronger pump tone incident on the JPA, allowing single-shot discrimination between the two cases [Fig. 1(c)].

The ability to better discern the qubit states with the JPA-backed readout is quantified by collecting statistics of single-shot measurements. The sequence used to benchmark the readout includes two measurement pulses, M_0 and M_1, each 700 ns long, with a central integration window of 300 ns [Fig. 2(a)]. Immediately before M_1, a π pulse is applied to Q_A in half of the cases, inverting the population of ground and excited state [Fig. 2(b)]. We observe a dominant peak for each prepared state, accompanied by a smaller one overlapping with the main peak of the other case. We hypothesize that the main peak centered at positive voltage corresponds to state $|00\rangle$, and that the smaller peaks are due to residual qubit excitations, mixing the two distributions. To test this hypothesis, we first digitize the result of M_0 with a threshold voltage V_{th}, chosen to maximize the contrast between the cumulative histograms for the two prepared states [Fig. 2(c)], and assign the value H (L) to the shots falling above (below) the threshold. Then we only keep the results of M_1 corresponding to $M_0 = H$. Indeed, we observe that postselecting 91% of the shots reduces the overlaps from ~6 to 2% and from ~9 to 1% in the H and L regions, respectively [Fig. 2(d)]. This substantiates the hypothesis of partial qubit excitation in the steady state, lifted by restricting to a subset of measurements where M_0 declares the register to be in $|00\rangle$. Further evidence is obtained by observing that moving the threshold substantially decreases the fraction of postselected measurements without significantly improving the contrast [$\sim +0.1(0.2\%)$ keeping 85 (13)% of the shots]. Postselection is effective in suppressing the residual excitation of any of the two qubits, since the $|01\rangle$ and $|10\rangle$ distributions are both highly separated from $|00\rangle$, and the probability that both qubits are excited is only ~0.2% [33]. Given the similarity between the two single-excitation histograms, the following experiments are performed by coherently manipulating Q_A only.

The performance of the JPA-backed readout and the effect of initialization by measurement are quantified by the optimum readout contrast. This contrast is defined as the maximum difference between the cumulative probabilities for the two prepared states [Fig. 3(a)]. Without

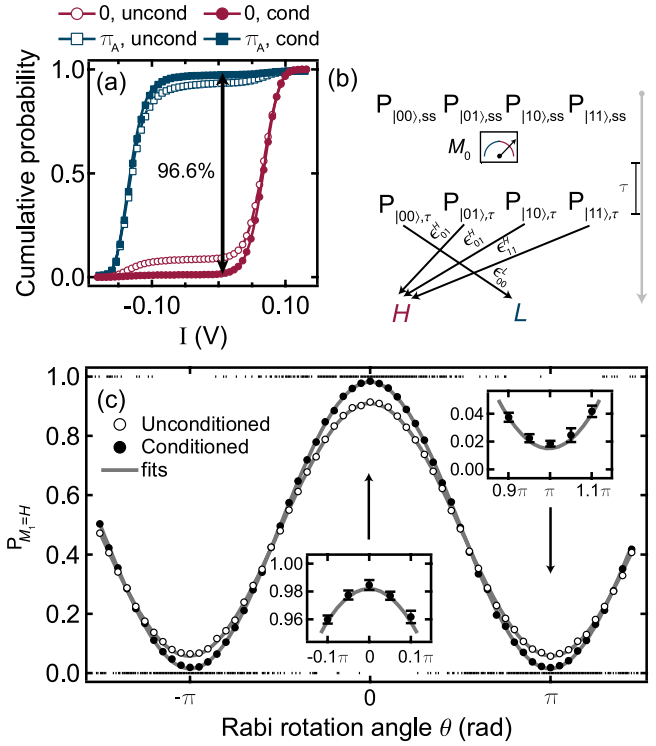

FIG. 3 (color online). Analysis of readout fidelity. (a) Cumulative histograms for M_1 without and with conditioning on $M_0 = H$, obtained from data in Figs. 2(c) and 2(d). The optimum threshold maximizing the contrast between the two prepared states is the same in both cases. Deviations of the outcome from the intended prepared state are: 8.9% (1.3%) for the ground state, 6.2% (2.1%) for the excited state without (with) conditioning. Therefore, initialization by measurement and postselection increases the readout contrast from 84.9% to 96.6%. (b) Schematics of the readout error model, including the qubit populations in the steady state and at $\tau = 2.4$ μs after M_0. Only the arrows corresponding to readout errors are shown. (c) Rabi oscillations of Q_A without (empty) and with (solid dots) initialization by measurement and postselection. In each case, data are taken by first digitizing 10 000 single shots of M_1 into H or L, then averaging the results. Error bars on the average values are estimated from a subset of 175 measurements per point. For each angle, 7 randomly chosen single-shot outcomes are also plotted (black dots at 0 or 1). The visibility of the averaged signal increases upon conditioning M_1 on $M_0 = H$.

initialization, the use of the JPA gives an optimum contrast of 84.9%, a significant improvement over the 26% obtained without the pump tone. Comparing the deviations from unity contrast without and with initialization, we can extract the parameters for the error model shown in Fig. 3(b). The model (see the Supplemental Material [33]), takes into account the residual steady-state excitation of both qubits, found to be ~4.7% each, and the error probabilities for the qubits prepared in the four basis states. Although the projection into $|00\rangle$ occurs with 99.8 ± 0.1% fidelity, this probability is reduced to 98.8% in the time $\tau = 2.4$ μs between M_0 and M_1, chosen to fully deplete the cavity of photons before the π pulse preceding M_1. We note that τ could be reduced by increasing κ by at least a factor of 2 without compromising T_{1A} by the Purcell effect [14]. By correcting for partial equilibration during τ, we calculate an actual readout fidelity of 98.1 ± 0.3%. The remaining infidelity is mainly attributed to qubit relaxation during the integration window.

As a test for readout fidelity, we performed single-shot measurements of a Rabi oscillation sequence applied to Q_A, with variable amplitude of a resonant 32 ns Gaussian pulse preceding M_1, and using ground-state initialization as described above [Fig. 3(c)]. The density of discrete dots reflects the probability of measuring H or L depending on the prepared state. By averaging over ~10 000 shots, we recover the sinusoidal Rabi oscillations without (empty) and with (solid) ground-state initialization. As expected, the peak-to-peak amplitudes (85.2 and 96.7%, respectively) equal the optimum readout contrasts in Fig. 3(a), within statistical error.

In an ideal projective measurement, there is a one-to-one relation between the outcome and the postmeasurement state. Such a measurement leaves the qubits in a known state, making it possible to perform subsequent quantum operations based on the outcome. We perform repeated measurements to assess the QND nature of the readout, following Refs. [34,35]. The correlation between two consecutive measurements, M_1 and M_2, is found to be independent of the initial state over a large range of Rabi rotation angles θ [see Fig. 4(a)]. A decrease in the probabilities occurs when the chance to obtain a certain outcome on M_1 is low (for instance to measure $M_1 = H$ for a state close to $|01\rangle$) and comparable to readout errors or to the partial recovery arising between M_1 and M_2. We extend the readout model of Fig. 3(b) to include the correlations between each outcome on M_1 and the postmeasurement state [33]. The deviation of the asymptotic levels from unity, $P_{H|H} = 0.99$ and $P_{L|L} = 0.89$, is largely due to recovery during τ, as demonstrated in Fig. 4(b). From the model, we extrapolate the correlations for two adjacent measurements, $P_{H|H}(\tau = 0) = 0.996 \pm 0.001$ and $P_{L|L}(\tau = 0) = 0.985 \pm 0.002$, corresponding to the probabilities that the pre- and postmeasurement state coincide. In the latter case, mismatches between the two outcomes are mainly due to qubit relaxation during M_2. Multiple measurement pulses, as well as a long pulse, do not have a significant effect on the qubit state [33], supporting the QND character of the readout at the chosen power.

We have implemented JPA-backed dispersive joint readout of transmon qubits in 3D circuit QED. The readout discriminates the two-qubit ground state from single-qubit excitations with 98.1% fidelity. This fidelity is limited by qubit relaxation, and we estimate that doubling T_1 will allow reaching the fault-tolerance threshold of 99% for surface-code error correction [27]. The QND character of

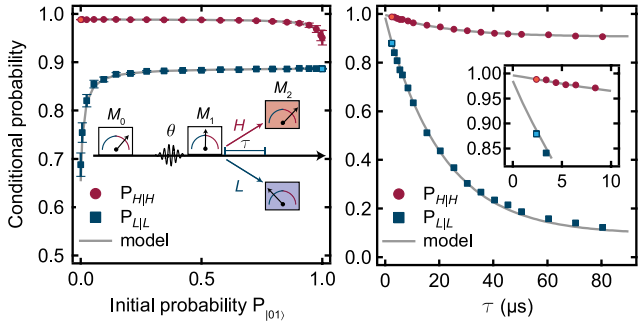

FIG. 4 (color online). Projectiveness of the measurement. (a) Conditional probabilities for two consecutive measurements M_1 and M_2, separated by $\tau = 2.4$ μs. Following an initial measurement pulse M_0 used for initialization into $|00\rangle$ by the method described, a Rabi pulse with variable amplitude rotates Q_A by an angle θ along the x-axis of the Bloch sphere, preparing a state with $P_{|01\rangle} = \sin^2(\theta/2)$. Dots (squares): probability to measure $M_2 = H$ (L) conditioned on having obtained the same result in M_1, as a function of the initial excitation of Q_A. Error bars are the standard error obtained from 40 repetitions of the experiment, each one having a minimum of 250 postselected shots per point. Deviations from an ideal projective measurement are due to the finite readout fidelity, and to partial recovery after M_1 [33]. The latter effect is shown in (b) where the conditional probabilities approach the unconditioned values, $P_H = 0.91$ and $P_L = 0.09$ for $\tau \gg T_1$, in agreement with Fig. 2, taking into account relaxation between the π pulse and M_2. Error bars are smaller than the dot size.

the readout allows us to demonstrate the simultaneous projection by measurement of two qubits into the ground state. Postselecting the measurement results, we correct residual single-qubit excitations, and prepare the register in $|00\rangle$ with 98.8% fidelity. Initialization will be imperfect when the population of the doubly excited state is relevant, but this problem can be addressed by choosing a different configuration of the joint readout that fully discriminates one of the computational states from the other three. Scaling to larger quantum registers, a few-percent excitation of each qubit will linearly decrease the probability of postselecting the ground state. An approach already taken [7] to suppress steady-state excitations is shielding the sample from infrared radiation. An all-together new strategy for initialization, enabled by the QND readout presented here, is to realize a feedback scheme wherein coherent operations on qubits depend on measurement results. For example, measuring a qubit and applying a π pulse conditioned on having projected onto the excited state can prepare the ground state deterministically on a time scale much shorter than T_1. Future experiments will also target the generation of entanglement by multiqubit parity measurement and feedback [36,37].

We thank F. Nguyen for discussions and experimental assistance, P. C. de Groot and M. Shakori for fabrication support, and R. N. Schouten and G. de Lange for electronics support. We acknowledge funding from the Dutch Organization for Fundamental Research on Matter (FOM), the Netherlands Organization for Scientific Research (NWO, VIDI Grant No. 680-47-508), the EU FP7 project SOLID, and the DARPA QuEST program.

Note added.—Recently, we became aware of a similar work by Johnson *et al.* [38] on preparation by measurement of one flux qubit.

[1] M. A. Nielsen and I. L. Chuang, *Quantum Computation and Quantum Information* (Cambridge University Press, Cambridge, England, 2000).
[2] T. D. Ladd, F. Jelezko, R. Laflamme, Y. Nakamura, C. Monroe, and J. L. O'Brien, Nature (London) **464**, 45 (2010).
[3] H. Paik *et al.*, Phys. Rev. Lett. **107**, 240501 (2011).
[4] A. Blais, R.-S. Huang, A. Wallraff, S. M. Girvin, and R. J. Schoelkopf, Phys. Rev. A **69**, 062320 (2004).
[5] A. Wallraff, D. I. Schuster, A. Blais, L. Frunzio, R.-S. Huang, J. Majer, S. Kumar, S. M. Girvin, and R. J. Schoelkopf, Nature (London) **431**, 162 (2004).
[6] A. Palacios-Laloy, F. Mallet, F. Nguyen, F. Ong, P. Bertet, D. Vion, and D. Esteve, Phys. Scr. **T137**, 014015 (2009).
[7] A. D. Córcoles, J. M. Chow, J. M. Gambetta, C. Rigetti, J. R. Rozen, G. A. Keefe, M. Beth Rothwell, M. B. Ketchen, and M. Steffen, Appl. Phys. Lett. **99**, 181906 (2011).
[8] K. Geerlings, S. Shankar, Z. Leghtas, M. Mirrahimi, L. Frunzio, R. J. Schoelkopf, and M. H. Devoret, Bull. Am. Phys. Soc. **57**, 1 (2012), http://meetings.aps.org/link/BAPS.2012.MAR.Z29.9.
[9] J. M. Chow *et al.*, arXiv:1202.5344 [Phys. Rev. Lett. (to be published)].
[10] P. Schindler, J. T. Barreiro, T. Monz, V. Nebendahl, D. Nigg, M. Chwalla, M. Hennrich, and R. Blatt, Science **332**, 1059 (2011).
[11] S. O. Valenzuela, W. D. Oliver, D. M. Berns, K. K. Berggren, L. S. Levitov, and T. P. Orlando, Science **314**, 1589 (2006).
[12] V. E. Manucharyan, J. Koch, M. Brink, L. I. Glazman, and M. H. Devoret, arXiv:0910.3039.
[13] M. D. Reed, B. R. Johnson, A. A. Houck, L. DiCarlo, J. M. Chow, D. I. Schuster, L. Frunzio, and R. J. Schoelkopf, Appl. Phys. Lett. **96**, 203110 (2010).
[14] A. A. Houck *et al.*, Phys. Rev. Lett. **101**, 080502 (2008).
[15] M. Mariantoni *et al.*, Science **334**, 61 (2011).
[16] V. B. Braginsky and F. Y. Khalili, Rev. Mod. Phys. **68**, 1 (1996).
[17] D. B. Hume, T. Rosenband, and D. J. Wineland, Phys. Rev. Lett. **99**, 120502 (2007).
[18] P. Neumann, J. Beck, M. Steiner, F. Rempp, H. Fedder, P. R. Hemmer, J. Wrachtrup, and F. Jelezko, Science **329**, 542 (2010); L. Robledo, L. Childress, H. Bernien, B. Hensen, P. F. A. Alkemade, and R. Hanson, Nature (London) **477**, 574 (2011).
[19] G. Nogues, A. Rauschenbeutel, S. Osnaghi, M. Brune, J. M. Raimond, and S. Haroche, Nature (London) **400**, 239 (1999); B. R. Johnson *et al.*, Nature Phys. **6**, 663 (2010); G. J. Pryde, J. L. O'Brien, A. G. White, S. D. Bartlett, and T. C. Ralph, Phys. Rev. Lett. **92**, 190402 (2004).

[20] H. M. Wiseman and G. J. Milburn, *Quantum Measurement and Control* (Cambridge University Press, Cambridge, England, 2009).
[21] S. Gleyzes, S. Kuhr, C. Guerlin, J. Bernu, S. Deléglise, U. Busk Hoff, M. Brune, J.-M. Raimond, and S. Haroche, Nature (London) **446**, 297 (2007).
[22] R. Vijay, D. H. Slichter, and I. Siddiqi, Phys. Rev. Lett. **106**, 110502 (2011).
[23] J. Gambetta, A. Blais, M. Boissonneault, A. A. Houck, D. I. Schuster, and S. M. Girvin, Phys. Rev. A **77**, 012112 (2008).
[24] Y. Matsuzaki, S. Saito, K. Kakuyanagi, and K. Semba, Phys. Rev. B **82**, 180518 (2010).
[25] F. Mallet, F. R. Ong, A. Palacios-Laloy, F. Nguyen, P. Bertet, D. Vion, and D. Esteve, Nature Phys. **5**, 791 (2009).
[26] B. Abdo, F. Schackert, M. Hatridge, C. Rigetti, and M. Devoret, Appl. Phys. Lett. **99**, 162506 (2011).
[27] D. S. Wang, A. G. Fowler, and L. C. L. Hollenberg, Phys. Rev. A **83**, 020302 (2011).
[28] M. A. Castellanos-Beltran, K. D. Irwin, G. C. Hilton, L. R. Vale, and K. W. Lehnert, Nature Phys. **4**, 929 (2008).
[29] R. Vijay, M. H. Devoret, and I. Siddiqi, Rev. Sci. Instrum. **80**, 111101 (2009).
[30] Q_A is a double-junction qubit with a random, nontunable magnetic flux offset placing it $\sim$1 GHz below its flux sweet spot, limiting its T_2^* [39]. The relatively short T_2^* of Q_B compared to [3] most likely results from qubit-frequency sensitivity to charge noise [39] and to photon number fluctuations arising from residual cavity excitation [40].
[31] D. I. Schuster *et al.*, Nature (London) **445**, 515 (2007).
[32] J. Majer *et al.*, Nature (London) **449**, 443 (2007).
[33] See Supplemental Material at http://link.aps.org/supplemental/10.1103/PhysRevLett.109.050507 for details on device fabrication, use of the JPA, and readout error model.
[34] A. Lupaşcu, S. Saito, T. Picot, P. C. de Groot, C. J. P. M. Harmans, and J. E. Mooij, Nature Phys. **3**, 119 (2007).
[35] N. Boulant *et al.*, Phys. Rev. B **76**, 014525 (2007).
[36] K. Lalumière, J. M. Gambetta, and A. Blais, Phys. Rev. A **81**, 040301 (2010).
[37] L. Tornberg and G. Johansson, Phys. Rev. A **82**, 012329 (2010).
[38] J. E. Johnson, C. Macklin, D. H. Slichter, R. Vijay, E. B. Weingarten, J. Clarke, and I. Siddiqi, preceding Letter, Phys. Rev. Lett. **109**, 050506 (2012).
[39] J. A. Schreier *et al.*, Phys. Rev. B **77**, 180502 (2008).
[40] C. Rigetti *et al.*, arXiv:1202.5533.